



Available online at [www.sciencedirect.com](http://www.sciencedirect.com)



EPSL

Earth and Planetary Science Letters 231 (2005) 131–146

[www.elsevier.com/locate/epsl](http://www.elsevier.com/locate/epsl)

## Abnormal monsoon years and their control on erosion and sediment flux in the high, arid northwest Himalaya

Bodo Bookhagen\*, Rasmus C. Thiede<sup>1</sup>, Manfred R. Strecker<sup>2</sup>

*Institut für Geowissenschaften, Universität Potsdam, Postfach 60 15 53, D-14415 Potsdam, Germany*

Received 18 June 2004; received in revised form 2 November 2004; accepted 17 November 2004

Available online 21 January 2005

Editor: E. Bard

---

### Abstract

The interplay between topography and Indian summer monsoon circulation profoundly controls precipitation distribution, sediment transport, and river discharge along the Southern Himalayan Mountain Front (SHF). The Higher Himalayas form a major orographic barrier that separates humid sectors to the south and arid regions to the north. During the Indian summer monsoon, vortices transport moisture from the Bay of Bengal, swirl along the SHF to the northwest, and cause heavy rainfall when colliding with the mountain front. In the eastern and central parts of the Himalaya, precipitation measurements derived from passive microwave analysis (SSM/I) show a strong gradient, with high values at medium elevations and extensive penetration of moisture along major river valleys into the orogen. The end of the monsoonal conveyer belt is near the Sutlej Valley in the NW Himalaya, where precipitation is lower and rainfall maxima move to lower elevations. This region thus comprises a climatic transition zone that is very sensitive to changes in Indian summer monsoon strength. To constrain magnitude, temporal, and spatial distribution of precipitation, we analyzed high-resolution passive microwave data from the last decade and identified an abnormal monsoon year (AMY) in 2002. During the 2002 AMY, violent rainstorms conquered orographic barriers and penetrated far into otherwise arid regions in the northwest Himalaya at elevations in excess of 3 km asl. While precipitation in these regions was significantly increased and triggered extensive erosional processes (i.e., debris flows) on sparsely vegetated, steep hillslopes, mean rainfall along the low to medium elevations was not significantly greater in magnitude. This shift may thus play an important role in the overall sediment flux toward the Himalayan foreland. Using extended precipitation and sediment flux records for the last century, we show that these events have a decadal recurrence interval during the present-day monsoon circulation. Hence, episodically occurring AMYs control geomorphic processes primarily in the high-elevation arid sectors of the orogen,

---

\* Corresponding author. Tel.: +49 331 977 2908.

E-mail addresses: [bodo@geo.uni-potsdam.de](mailto:bodo@geo.uni-potsdam.de) (B. Bookhagen), [thiede@geo.uni-potsdam.de](mailto:thiede@geo.uni-potsdam.de) (R.C. Thiede), [strecker@geo.uni-potsdam.de](mailto:strecker@geo.uni-potsdam.de) (M.R. Strecker).

<sup>1</sup> Tel.: +49 331 977 2908.

<sup>2</sup> Tel.: +49 331 977 5261.

while annual recurring monsoonal rainfall distribution dominates erosion in the low- to medium-elevation parts along the SHF.

© 2004 Elsevier B.V. All rights reserved.

**Keywords:** Asian monsoon; precipitation; Himalayas; debris flows; landscape evolution

## 1. Introduction

Climate change, climate variability, and short-lived extreme weather events exert control on hillslope and transport processes, and hence profoundly impact character and rates of surface processes and therefore landscape development [1–6]. Along the Southern Himalayan Mountain Front (SHF), interannual variations in Indian Summer monsoon strength strongly influence sediment flux and river discharge to the foreland [7–9]. However, the link between precipitation distribution, erosional hillslope processes (e.g., landsliding, debris flows), and sediment transport in the mountainous regions along the SHF is poorly constrained, and the impact of short-lived, abnormal monsoon events on landscape evolution has not been quantified. This is important, because voluminous debris flows, rock falls, slope failures, and massive effects on infrastructure document a link between short-lived climate and surface-process phenomena. Particularly in high mountain terrains, a better assessment and understanding of the connection between extreme climatic events and surface-process response is desirable, but often difficult to achieve due to the lack of adequate monitoring possibilities. A synoptic comparison of rainfall data and its spatial variability in remote mountainous regions can be accomplished, however, by using high-resolution, satellite-borne passive microwave data.

In this study we show that the Sutlej Valley region ( $78^{\circ}\text{E}$ ,  $31^{\circ}\text{N}$ ) of the northwest Himalaya comprises a climatic transition zone that is very sensitive to the strength of the Indian Summer Monsoon (ISM). The availability of rain-gauge, discharge and suspended sediment-flux data makes this region an ideal environment to study the impacts of monsoonal precipitation on landscape-shaping processes. We processed and calibrated passive microwave data of the last decade to constrain temporal and spatial variations in rainfall and identified an abnormal monsoon year (AMY) in

2002. During the 2002 monsoon season, exceptionally strong rainfall events that were not observed in the last decade affected the usually arid, high-elevation regions of the upper Sutlej Valley. In this orographically shielded region, sediment production and mean basin denudation rates are low during the presently weak ISM circulation. Only during AMYs moisture penetrates farther into the orogen, amplifies erosive hillslope processes, such as debris flows, and increases fluvial sediment flux. In order to quantify the effect of shifting precipitation patterns on landscape evolution, we analyzed river discharge, sediment transport, and rainfall measurements, as well as satellite imagery before and after the AMY 2002 monsoon season.

Our results show a pronounced increase in mean basin denudation rates for these abnormal, recurring events. More importantly, amplified erosive hillslope processes that were triggered during AMYs dominate channel formation and fluvial network evolution in the arid, high-elevation sectors. While sediment efflux from this orographically shielded region was enhanced, total sediment flux toward the Himalayan foreland is still controlled by erosion of topographically forced rainfall in the large monsoonal belt along the SHF. Thus, the present-day weak monsoon circulation mainly affects areas between 1 and 3 km elevations. However, studies of proxies for monsoonal precipitation distribution strongly suggest enhanced orogenward moisture migration into the high, arid regions in the late Pleistocene and early Holocene [10,11]. During these periods, sediment flux toward the Himalayan foreland and adjacent oceans may have been dominated by material that was easily eroded from the shielded, high-elevation sectors. In this paper, we explore the geomorphic processes and influence on sediment flux on annual and event timescales to document the importance of AMYs on landscape-shaping processes.

## 2. The Indian summer monsoon (ISM)

The ISM is part of a larger phenomenon called the InterTropical Convergence Zone (ITCZ). The ITCZ separates the wind circulation of the northern and southern hemispheres [12,13]. This zone migrates north and south with the annual changes of the sun's declination and is located where the NE and SE trade winds converge. It is also characterized by strong upward motion of air and heavy, convective rainfall, as a result of intense solar heating during the boreal summer. The high topography of the Tibetan Plateau and latent heat released by the condensation of moisture amplifies the relative warming of the Asian landmass compared to the surrounding oceans and hence helps to establish the ISM circulation (e.g., [12,14]). Interannual variations of ISM strength mainly result from deflections of this thermal gradient (e.g., through sea-surface temperatures during El Niño/Southern Oscillation and Asian winter snow cover distribution; e.g., [14–16]). General moisture transport during the ISM is controlled by the strong thermal divergence caused by the low-pressure cell over the Tibetan Plateau and high-pressure over the surrounding oceans, producing north- to northwestward, counterclockwise humid eddies originating in the Bay of Bengal (e.g., [14,17,18]). The monsoonal vortices are deflected and swirl along the SHF to the northwest, causing heavy monsoonal precipitation from convection cells, when colliding with the mountain front (Fig. 1).

Primary control on the path of the monsoonal vortices and hence, moisture transport, is guided by the prevailing wind direction and speed during the ISM [18]. However, on medium to small spatial scales ( $10^2$ – $10^4$  km $^2$ ), local topography governs moisture migration along topographic barriers and into deeply incised valleys perpendicular to the mountain front (Fig. 1). The influence of orography can be attributed primarily to localized disturbances of the vertical structure of the atmosphere. Such disturbances exert important control, acting either as barriers, elevated heat sources, and sinks, or as concentrated areas of high roughness (e.g., [19,20]). In addition to destabilizing the atmosphere, airflow over such topographic barriers leads to the ascent of relatively water-rich warm air from lower elevations. The forced ascent of moist air enhances condensation, the formation and

growth of clouds, and ultimately, controls the triggering, duration, and intensity of precipitation events at high elevations. For example, the E–W-oriented Shillong Plateau located to the south of the SHF forms a ~2-km-high barrier, which forces high amounts of rainfall (~5 m/yr) on the south, whereas leeward areas along the SHF receive ~1 m/yr (Fig. 1). During the ISM, condensation on the windward side is initiated when a wet air parcel from the Bay of Bengal can no longer hold water in the vapor phase. As moisture-rich air masses move up in the atmosphere along the orographic barrier, pressure decreases and volume expands. Simultaneously, temperature and saturation vapor pressure decrease due to the conservation of energy and the proportionality between pressure and temperature of an ideal gas (e.g., [19]). This interplay between low-level moist air flows and topography controls the amount and distribution of rainfall. Comparable conditions, although with lower amounts of precipitation, exist along the entire SHF.

The high rainfall amounts during the ISM thus exercise strong control on river discharge and consequently sediment transport, leading to major flooding and sediment deposition south of the orographic barriers.

### 2.1. Determining precipitation from passive microwave data

To constrain the amount and distribution of rainfall in the Himalaya, and particularly the Sutlej region with sufficiently high resolution, we used passive microwave data from the Special Sensor Microwave/Imager (SSM/I) of the polar-orbiting Defense Meteorological Satellite Program (DMSP). The SSM/I satellite, which has been in operation since 1987 [21], has the unique ability to penetrate through cirrus clouds and sense the emitted and scattered radiation caused by raindrops and precipitation-sized ice particles, respectively. In the early stages of SSM/I data analysis, studies were limited to oceanic regions because the determination of rainfall by passive microwave measurements is based on low-frequency/emission techniques, and hence estimation was more direct over ocean than over land. In this study, however, high-frequency/scattering techniques are used. The primary method for land-rainfall

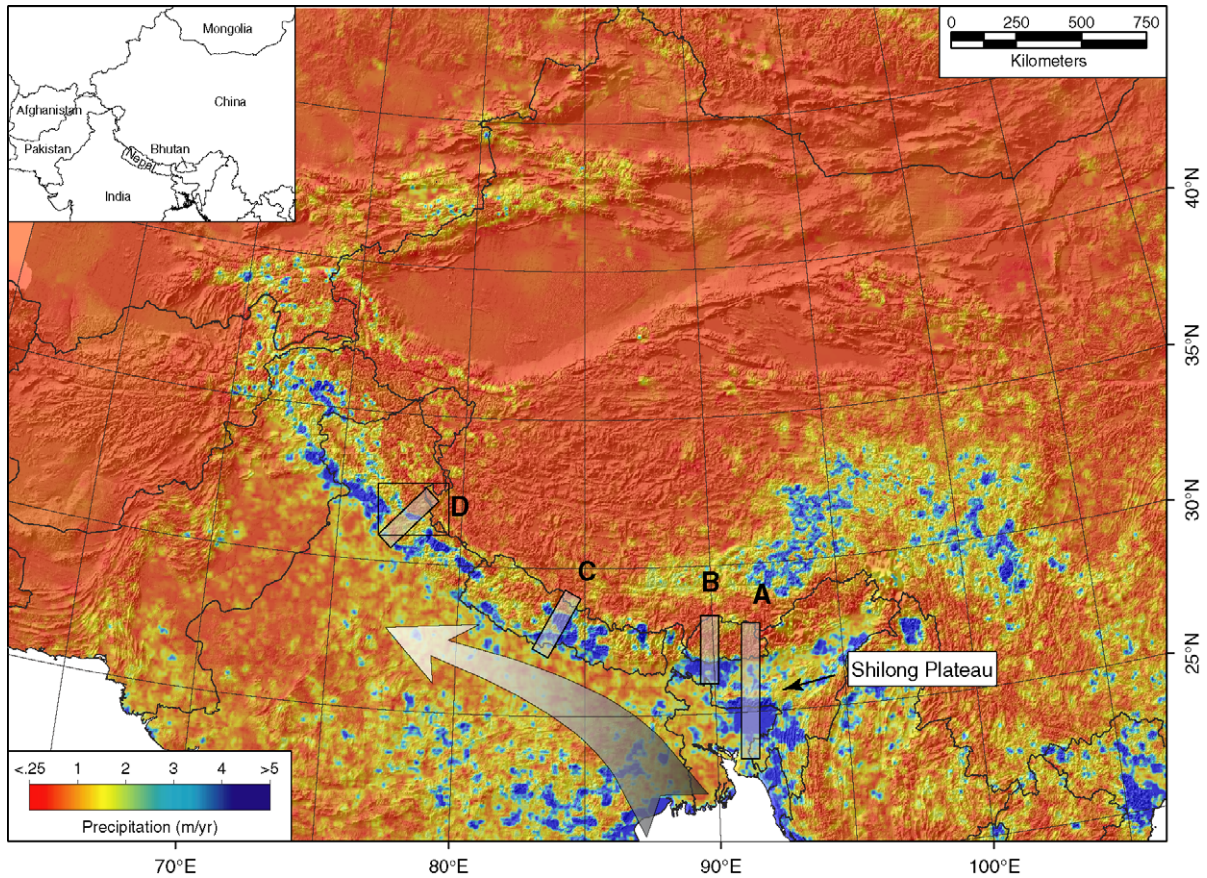


Fig. 1. Mean annual precipitation for the Himalayan region based on passive microwave SSM/I data, analyzed for a 10-yr time period (1992–2001, where data were available) during the Indian Summer Monsoon (June–August). Large arrow indicates moisture transport from the Bay of Bengal along the Southern Himalayan Front. Swath profiles (Fig. 2) are outlined by black boxes with gray shading. Profiles (from E to W) are: (A) Shillong-Plateau and Eastern Bhutan, (B) Sankosh River in Western Bhutan, (C) Kali Gandaki River in Central Nepal, and (D) Sutlej River, NW Himalaya. Plain, black box indicates location of Fig. 3.

retrieval uses an 85 GHz scattering-based algorithm (e.g., [22–25]) to obtain daily land precipitation with a spatial resolution of 156.25 km<sup>2</sup> (footprint of 12.5 km). The rain signature needs to be separated from other surfaces exhibiting similar characteristics, such as snow cover, deserts and semiarid regions [22,26]. Overviews of the varying techniques for rainfall retrieval from the SSM/I are presented by [27,28]. Many of the algorithms suffered from the improper delineation of rain areas from other surfaces that exhibit similar microwave signatures, resulting in erroneous excessive monthly rainfall amounts (e.g., [26]). To avoid these problems, we identified critical regions such as glaciers, ice, and snowfields using screening techniques suggested by Grody [22]. In

addition, we applied a supervised classification algorithm on a Landsat TM mosaic for the complete Himalayan region to determine these critical areas more reliably. We then processed the marked regions in a different way by taking into account the surface characteristics.

We focused on processing data for the summer monsoon months because more than 80% of precipitation along the SHF falls during the ISM [17]. In addition, the increased snow cover during winter would necessitate extensive screening to distinguish snow from overland precipitation. Where available, we analyzed data for the three summer monsoon months (June–August) between 1992 and 2002 (Fig. 1). This information was first calibrated with local

rainfall measurements from the northwest Himalaya (Beas Bakhra Management Board, B.B.M.B. and Jaiprakash Company Ltd.). In order to understand and quantify precipitation changes along the SHF, we compare our calibrated data with gauge stations in a similar remote environment in central Nepal [18,29] (Fig. 2). Although the datasets are spatially inconsistent (point measurement vs. corresponding SSM/I grid cell of approx. 150 km<sup>2</sup>), they still demonstrate the validity of the applied remote-sensing technique. Precipitation in these areas is strongly dependent on elevation and thus we plot the ratio of precipitation amount and elevation for both datasets (Fig. 2 and additional information in the electronic Appendix). The rain gauges in central Nepal document a nocturnal peak [29], which is not reflected in the SSM/I data because of limited temporal coverage. We emphasize that errors of 15–35% are associated with total precipitation amounts, while relative values are more accurate. Low precipitation values (<300 mm/yr) are associated with larger errors due to the interference from screening algorithms, whereas medium to high precipitation (approx. >750 mm/yr) from convection cells is very well represented. Precipitation in the Himalayan foreland may be underestimated because it can be forced by very small

convection cells with strong vertical velocity fields that are not correctly represented by the scales used in this study (e.g., [18]). Furthermore, the contribution of stratiform precipitation is larger, characterized by widespread slow ascent velocity fields, which is not very accurately captured with passive microwave analysis. For these reasons, we focus on the valley- and orogen-scale moisture transport, where precipitation from heavy convection cells is the predominant rain type.

We extended our decadal dataset to the middle of the last century using rain-gauge observations in the vicinity of the Sutlej River region with the Global Historical Climatologic Network (GHCN Version 2) [30] and stations maintained by the B.B.M.B. (personal communication, 2003). In addition, daily suspended sediment transport and river discharge measurements are available at a few stations along the Sutlej River and also along the Baspa River, a major tributary in the transitional zone between the humid and arid parts of the orogen (B.B.M.B. and Jaiprakash). The Baspa gauge data covers 35 yr of measurements, while data along the main stem only provide a 20-yr record. These data were used to calculate sediment flux and mean basin denudation rates. Daily suspended sediment transport in mg/l is

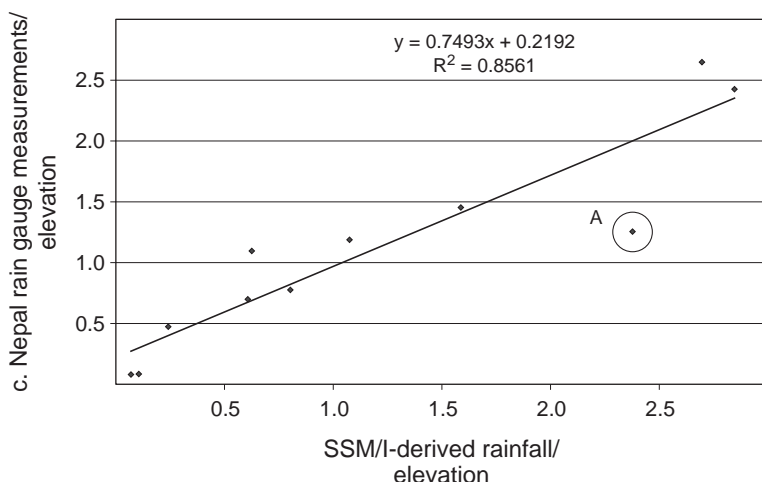


Fig. 2. Ratios of rainfall estimations and elevation. We plot the ratio of central Nepal rain gauges and elevation (see [18] and electronic Appendix for more information) vs. the ratio of SSM/I-derived rainfall and elevation for the same time interval (June to September, 1999 and 2000). We average all measurements from spot gauges that lie within the ~150 km<sup>2</sup> SSM/I grid cell and divide it by the averaged elevation. The datasets show a good correlation despite their different spatial resolutions. A circled outlier labeled A (included into the regression analysis) is caused by a different grid cell elevation and not by a significant difference in rainfall amount (rain gauge elevation of ~1300 m asl with 1627 mm/yr vs. 750 m asl and 1790 mm/yr of the SSM/I grid cell).

available during the ISM months, while measurements during winter indicate very low values. Bedload transport has been neglected because studies in similar partially glaciated, steep environments show that the total transported sediment amount consists only of 6% bedload [31]. However, bedload transport rates are difficult to measure and we thus consider our erosion rates to be only minimum values.

ASTER (Advanced Spaceborne Thermal Emission and Reflection Radiometer) satellite images taken before and after the 2002 AMY were used to identify reactivated and newly formed channels on hillslopes. We analyzed the three visible bands (VNIR) of the ASTER sensor. This data is highly correlated and we used Principal Component Analysis (PCA) to transform the different bands to a set of uncorrelated output bands, which are ordered by decreasing variability. The main use of PCA is to reduce the dimensionality while retaining as much information as possible (e.g., [32]). This step was taken to minimize the divergence in surface reflectance because the ASTER images were taken at different seasons and times of day. We filtered and removed homogenous regions with non-relevant information (i.e., glaciers and shadows from surrounding mountains) to enhance contrast, thus making it easier to locate changes between satellite images, taken before and after the 2002 AMY.

## 2.2. Moisture transport and precipitation gradients during the ISM

We identified two precipitation gradients that fundamentally influence vegetation and erosional geomorphic processes along the SHF. Precipitation gradually decreases with distance from the Bay of Bengal (from E to W) and decreases leeward of orographic barriers, toward the Tibetan Plateau (from S to N). To illustrate the topographic control on precipitation, four representative swath profiles perpendicular to the Himalayan orogen were created (Fig. 3). The Shillong Plateau (~1.5 km) constitutes the most prominent orographic barrier (Figs. 1 and 3A). The southern flank of the plateau is the wettest inhabited place on earth (Cherrapunji, District Meghalaya) at 1300 m asl with a record of 9.3 m rainfall during 1 month in July 1861 (Indian Meteorological Department). An orographic rain shadow thus exists and results in much drier

conditions to the north of the Shillong Plateau in E Bhutan compared to regions to the east and west along the SHF. In contrast, rainfall in the Sankosh Valley region of W Bhutan (Fig. 3B) just to the W of the dry part along the SHF receives high precipitation (~3.5 m/yr) with maximum amounts of up to 5 m/yr. There precipitation is forced by low to medium elevations of 0.5 to 2 km. Moisture transport in the Kali Gandaki region (central Nepal, Fig. 2C) is strongly controlled by valley topography. Medium amounts of rain (~2.3 m/yr) are forced on the SHF, whereas moisture migrates into the orogen through the Kali Gandaki River to the E of the swath profile (Fig. 1). Here, wet air condenses on the orographic barrier to form a second precipitation peak at ~150 km north of the mountain front (Fig. 3C). Interestingly, heavy, wet air masses do not easily overcome moderately elevated ranges, similar to the orographic barrier of the Shillong Plateau (Fig. 3A). Above a mean elevation of 3 km asl, precipitation decreases and north of the main Himalayan barrier, with peaks above 5 km, very little precipitation is observed (Fig. 3B,C). Therefore, during summer under present conditions, moisture only reaches the dry Tibetan Plateau primarily by migrating upstream through river valleys, thereby circumventing orographic obstacles (Fig. 1).

In contrast to the high amounts of precipitation in the eastern and central parts of the SHF, rainfall in the Sutlej Valley region is characterized by lower ISM precipitation and maxima at lower elevations (Fig. 3D). Moisture migrates along the valley to condensate along the main topographic barrier at moderate altitudes of about 2.5 km asl (Fig. 4A). There, the decadal SSM/I-derived ISM mean rainfall does not exceed 1.5 m/yr and regions to the NE are left dry (<0.3 m/yr). For example, the village of Sangla in the Baspa Valley is in a semi-arid corridor where rain-gauge measurements result in ~0.2 m/yr during the ISM of the last decade. However, during the 2002 AMY, precipitation migrated farther into the orogen and increased rainfall amounts up to ~0.8 m/yr in the Baspa Valley (Figs. 3D and 4B). Interannual variations in precipitation and resulting river discharge in the study region during the last decade were not subject to large amplitude changes (Fig. 5). There exists a large, but constant offset between the rain-gauge data and SSM/I precipitation estimates. Similar

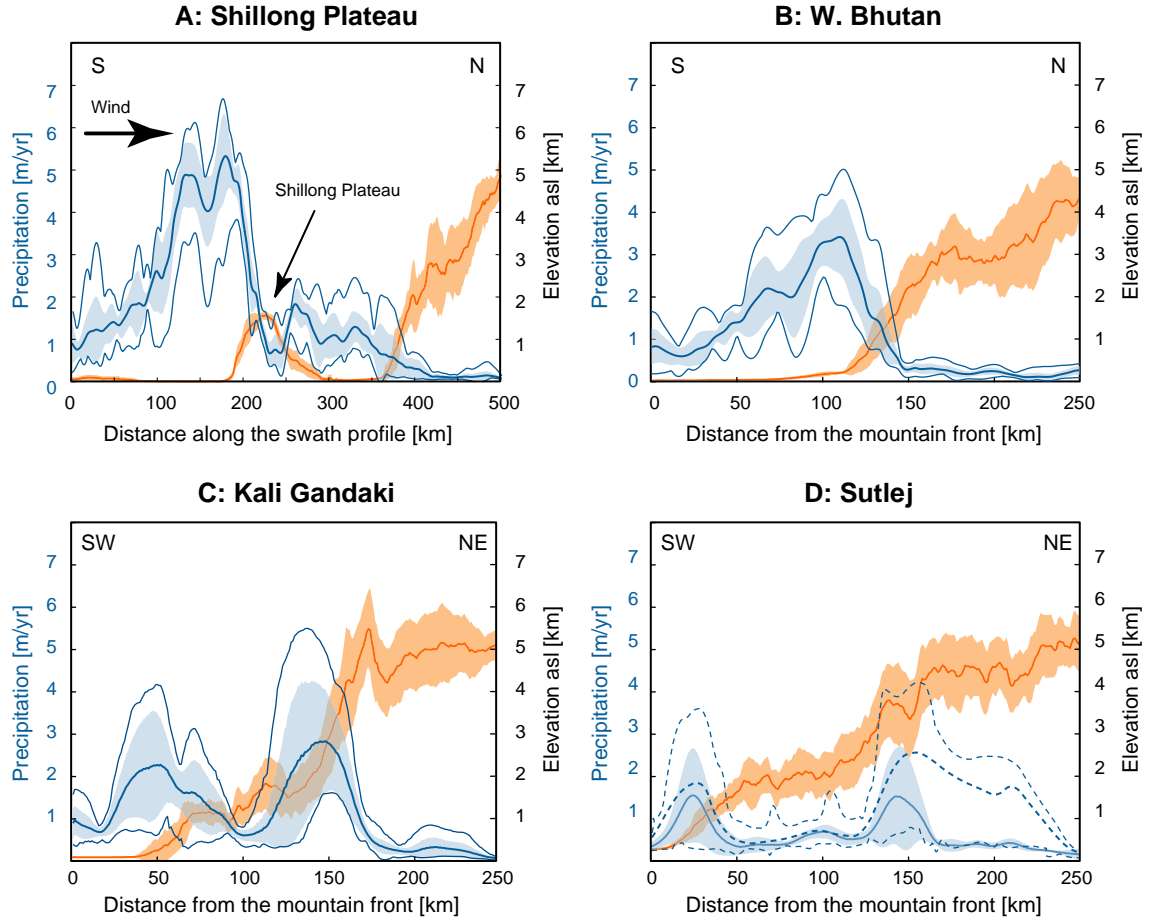


Fig. 3. Topographic and precipitation swath profiles, see Fig. 1 for locations. Swath profiles are 80 km wide and centered along river valleys, perpendicular to the mountain front. Topography (orange) derived from HYDRO1K dataset (USGS) and precipitation (blue) from passive microwave data. Bold lines indicate mean values, shading denotes  $\pm 2\sigma$  ranges, and thin lines minimum and maximum annual rainfall. Prevailing wind direction during monsoon season is from S–SE to N–NW. Note high amounts of rainfall on the windward side of orographic barriers. Along the Sutlej Valley, bold dashed line indicates annual precipitation during the 2002 AMY and thin dashed lines minimum and maximum values.

to observation in central Nepal, we assume that most of the rainfall occurred at high elevations on the hillslopes [29]. Thus gauge stations along the valley bottom that were used to calibrate passive microwave data do not capture the orographic rainfall effects. However, SSM/I rainfall integrated over the catchment area shows a linear correlation with discharge measured in the Baspa River near Sangla (see information in the electronic Appendix). Mean SSM/I ISM rainfall for the Sangla grid-cell during the last decade was 0.65 m/yr and increased to 1.5 m/yr during the 2002 AMY (Fig. 5).

The rainfall anomaly map (Fig. 4C) clearly demonstrates that wet air traveled along river valleys to bypass orographic barriers and reach scarcely vegetated, normally arid regions ( $<0.3$  m/yr rain) of the internal part of the Himalaya. For example, rainfall migrated along the Chandra and Bhagirati rivers to reach the Baspa River and the upper Spiti River, two major tributaries of the Sutlej (Fig. 4C). In these areas, heavy rainstorms in late August and September of the 2002 AMY amplified river discharge and sediment flux while moisture precipitated at high elevations along the windward sides of topographic barriers. Thus, the arid,

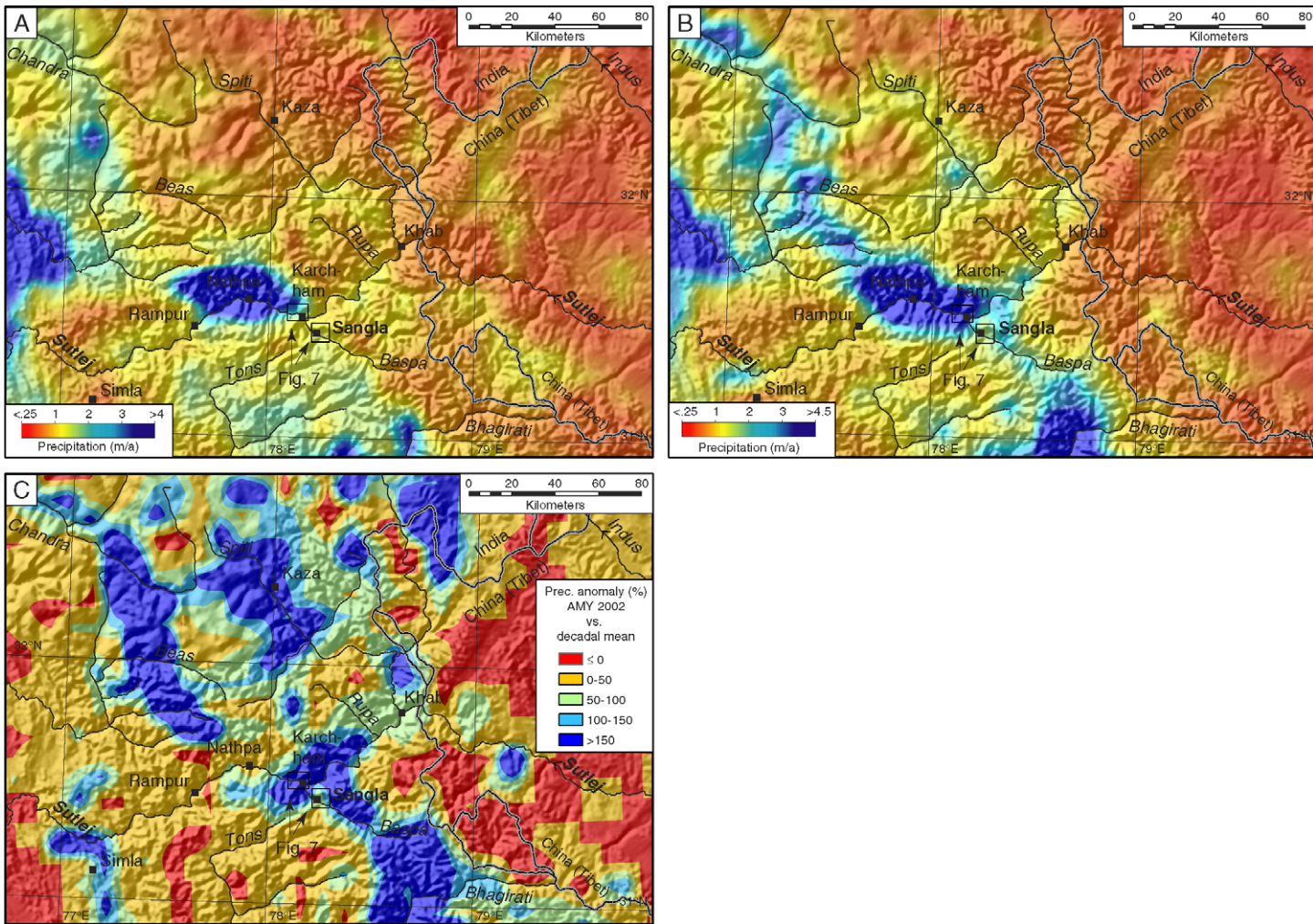


Fig. 4. Mean ISM precipitation and shaded relief of the Sutlej River region. Topography is based on GTOPO30 (USGS), and precipitation was derived from calibrated SSM/I passive microwave data that were smoothed for this output. (A) Normal monsoonal precipitation distribution (based on averaged 10-yr analysis); (B) abnormal monsoon year (AMY) of 2002 (averaged for 3 months, where data available); (C) precipitation anomaly map (in percent) showing the magnitude changes between decadal mean and 2002 AMY. Positive anomalies depict more rain during the 2002 AMY, i.e. a 100% anomaly represents the double amount of precipitation. The dominant effect of topography on precipitation distribution is best demonstrated in the middle region of the Sutlej Valley, where moderate amounts of precipitation ( $\leq 3$  m/yr) fall in convective cells. Only during the 2002 AMY moist air masses penetrate northeastward into the orogen through the Beas, Chandra, and Bhagirati valleys, and generate greater amounts of precipitation in the commonly dry areas of the Spiti, Baspa, and Sutlej rivers. Black box outlines region of Fig. 7.

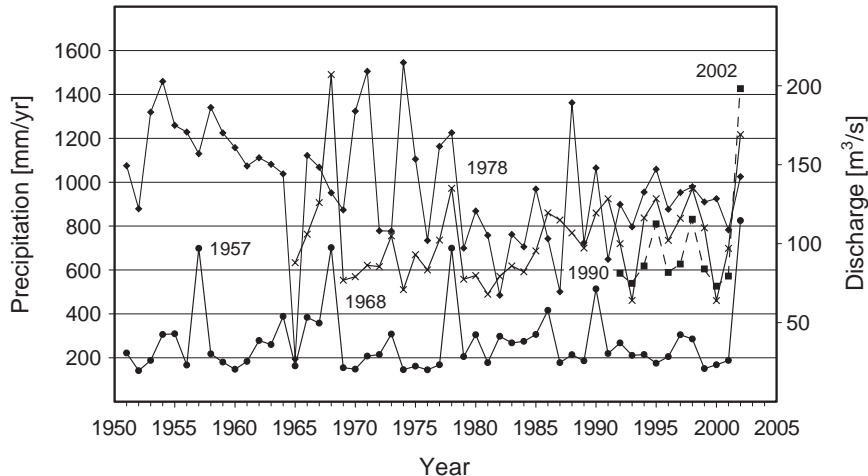


Fig. 5. Rain-gauge measurements (-●-) and SSM/I precipitation (-■-) for the village of Sangla (Baspa Valley). Simla rain-gauge data is shown as a representative station for the low- to medium-elevation regions (-◆-). Mean annual Indian Summer Monsoon (ISM) rainfall for Sangla is low ( $\sim 0.28 \text{ m/yr}$ ) during the last 50 years but indicate AMYs in 1957, 1968, 1978, 1990, and 2002. Baspa River discharge (- $\times$ -) since 1965 shows similar events. Mean ISM SSM/I rainfall is  $0.65 \text{ m/yr}$  in the vicinity of the village Sangla during the last decade, while AMY estimations are significantly increased.

high-elevation regions received precipitation in excess of 200% of the annual mean during non-AMY years (Fig. 4C). We thus expect the geomorphic response (e.g., erosional hillslope processes) and resulting sediment transport to be much more pronounced during such extreme climatic, abnormal years. In contrast, rainfall in the low- and medium-elevation regions (<3 km asl) was only moderately enhanced by about 25–50%. Although we cannot precisely reconstruct spatial migration of moisture for the time predating SSM/I measurements, we were able to identify the same contrasting pattern throughout the last 50 yr using rain gauges in the Sutlej Valley (B.B.M.B. and Jaiprakash Ltd.) and adjacent regions [30].

On a synoptic scale we are able to define two compartments of monsoonal precipitation: High rainfall amounts along the orographic barriers of the SHF and moderate amounts in the Indian plains to the south. While precipitation patterns in the lowlands are extensively covered by investigations by Shrestha [17] and Parthasarathy et al. [33], we concentrated on areas affected by orographic rainfall. These regions have not received much attention, and precipitation quantification is restricted to a limited number of local studies because of the lack of adequate data (e.g., [18,29]). It is noteworthy that the two rain compartments show very different behavior with respect to the

interannual variations and precipitation distribution during the ISM circulation. For example, the 2002 AMY was characterized by a negative rainfall anomaly over the Indian plains, whereas the arid mountainous regions were affected by torrential rainfall and major flooding (Fig. 4; International Red Cross Annual Report, 2002; Indian Meteorological Department; United Nations Office for the Coordination of Humanitarian Affairs (OCHA)). In addition, the onset of the ISM in 2002 was delayed by several weeks, before violent, active monsoon phases transported moisture from the Bay of Bengal to the Indian plains and the SHF. Hence, a first order control on rainfall amount on the Indian continent is exerted by large-scale atmospheric modulations (e.g., in relation to ENSO) and changes in sea surface temperatures (e.g., [12,15,17,34]), while tectonically created topography plays an important role in forcing and focusing orographic rainfall. Interestingly, precipitation patterns caused by orographic forcing along large river valleys in the medium elevations of the SHF have remained rather stationary during at least the last decade despite high ISM-strength variations. Thus, precipitation as an effective erosion agent might have played a significant control on localized denudation along the medium-elevation sectors of the SHF on geologic time scales (e.g., [35,36]).

### 2.3. Precipitation patterns, erosional hillslope processes, and sediment flux in the northwest Himalaya

The significantly different spatial distribution of precipitation during an abnormal monsoon year derived from high-resolution passive microwave data (Fig. 4C) can be used to further explore the links between erosional hillslope processes and strong rainfall events. In semi-arid to arid mountainous environments, high-magnitude, low-frequency events commonly dominate both river-channel processes and hillslope erosion (e.g., [37–39]). Consequently, during extreme climatic events, the relations between high precipitation and hillslope processes, channel erosion, and sediment transport play a fundamental role in shaping arid, mountainous landscapes. However, only few studies have been published that illustrate impacts of high intensity rainfall events on channels in such environments (e.g., [3]); in fact, knowledge about erosion processes taking place during abnormal strong events is very limited and often based on deduction. Here, we combine field and satellite observations, river discharge data, information on sediment flux, and precipitation measurements during the 2002 AMY to identify processes leading to enhanced hillslope erosion during strong climatic events.

The Sutlej River is an integral part of the Indus catchment and comprises the third largest drainage area in the Himalaya and southern Tibet. Before entering India, it drains 43,500 km<sup>2</sup> on the Tibetan Plateau. However, due to the aridity in Tibet, this large drainage-basin area does not result in significant discharge and sediment flux into the Himalayan region. In crossing the regions of the Tethyan sediments, Higher and Lower Himalayan Crystalline sectors, and units of the Lesser Himalaya, the Sutlej River rapidly descends from almost 4 km to 0.2 km asl in the Himalayan foreland. Along its course, transient climatic and related geomorphic boundaries exist that develop in response to the changing monsoonal conditions. Thus, depending on the strength and stage of the ISM, characteristic landscape compartments evolve with highly divergent rainfall, vegetation cover, and hillslope processes.

We distinguish between the humid, low- to medium-elevation parts (1~2.5 km asl) that are characterized by high-sediment production (HSP)

during high-frequency/low-magnitude rainfall events, and the upstream, arid, high-elevation regions ( $>\sim 3$  km asl) defined by low-sediment production (LSP) during normal ISM years. During these typical monsoon years, mean ISM daily river discharge and sediment load in the Sutlej at Rampur (HSP) are on the order of 800 m<sup>3</sup>/s and 2.5 g/l (Table 1). Here, and approximately 60 km upstream, erosional hillslope processes during the monsoon season dominate mass wasting into the channels, and sufficient runoff ensures sediment removal (e.g., [7–9]).

In contrast, mean ISM river discharge and silt load in the LSP area at Khab, south of the Sutlej–Spiti confluence, are  $\sim 225$  m<sup>3</sup>/s and  $\sim 0.15$  g/l, respectively. Thus, regions along the Sutlej Valley that are always exposed to the high ISM rainfall regime show constantly high sediment flux (Table 1). During the 2002 AMY, precipitation increased only by a small percentage in these sectors (Fig. 4C) and did not result in significantly enhanced sediment transport. The humid, HSP compartment with mean elevations between 1 and 2.5 km thus tends to compensate slightly higher rainfall. In contrast, the Baspa River basin is located in the LSP, high-elevation semi-arid region ( $>\sim 3$  km asl). It has a 35-yr average ISM discharge (excluding AMYs) of 96 m<sup>3</sup>/s ( $2\sigma: \pm 20$  m<sup>3</sup>/s), while the 2002 AMY is characterized by  $\sim 169$  m<sup>3</sup>/s (Fig. 5; Table 1). Sediment load measurements in the Baspa River show similar distinctions from 0.95 g/l and  $\sim 1.23$  g/l during the 2002 AMY (Jaiprakash Ltd., unpublished company data). These values are mean ISM (June–August) amounts based on daily measurements—extreme events after heavy rainstorms can have significantly higher values and exert a crucial control on the amount of evacuated sediment. The 2002 AMY value is also a minimum estimation, because daily measurements were difficult to obtain and were not collected during and after heavy rainstorms while rivers were flowing rapidly. However, we expect transported grain sizes to be significantly larger during the AMY 2002 when peak discharges of up to 500 m<sup>3</sup>/s must have significantly increased the shear stress acting on the riverbed to overcome the threshold of motion (e.g., [4]).

In order to calculate annual sediment transport rates for the Baspa basin, we multiply river discharge (96 m<sup>3</sup>/s) and suspended sediment flux (0.95 g/l) for

Table 1

Summary of precipitation, discharge, and suspended sediment flux data for the Sutlej Valley region during normal monsoon conditions and the abnormal monsoon year (AMY) 2002

	'Normal' monsoon conditions		AMY 2002	
	High-sediment production (HSP)	Low-sediment production (LSP)	High-sediment production (HSP)	Low-sediment production (LSP)
Rainfall [m/yr] <sup>a</sup>	1.5	0.3	1.7	0.75
JJA-monsoon average discharge [m <sup>3</sup> /s]	Nathpa (Sutlej) 790±10 <sup>b</sup> Rampur (Sutlej) 850 ±130 <sup>g</sup>	Khab (Sutlej) Sangla (Baspa) Karchham (Sutlej)	~225 <sup>c</sup> 96±20 <sup>d</sup> 380±24 <sup>c</sup>	Nathpa (Sutlej) ND Khab (Sutlej) Sangla (Baspa) Karchham (Sutlej) ND
JJA-monsoon suspended sediment flux [g/l]	Nathpa (Sutlej) 1.7±0.3 <sup>b</sup> Rampur (Sutlej) 2.5±0.8 <sup>g</sup>	Khab (Sutlej) Sangla (Baspa) Karchham (Sutlej)	~0.15 <sup>c</sup> 0.95 ±0.15 <sup>g</sup> 1.2±0.3 <sup>c</sup>	Nathpa (Sutlej) ND Khab (Sutlej) Sangla (Baspa) Karchham (Sutlej) ND

High-sediment production (HSP) region denotes the area between 1 and 2.5 km elevation, while the low-sediment production (LSP) region lies above 3 km elevation leeward of orographic barriers. Measurements from Sangla, Baspa were taken from Jaiprakash Hydroelectric Power Industries Lim., other data is from the B.B.M.B. (Beas Bhakra Management Board). Standard deviations are given in 2σ; ND indicates no data was available; JJA stands for June, July, August.

<sup>a</sup> Rainfall based on calibrated passive microwave data (SSM/I) from 1992 to 2001 and 2002, respectively.

<sup>b</sup> Based on a 21-yr record from 1970 to 1990.

<sup>c</sup> Based on an 11-yr record from 1970 to 1980.

<sup>d</sup> Abnormal monsoon years (AMYs) as identified in Fig. 5 were excluded from the calculations.

<sup>e</sup> Average discharge for 1968, 1978, 1990 and 2002 AMYs is 159±41 m<sup>3</sup>/s.

<sup>f</sup> Measurements were not taken continuously throughout 2002.

<sup>g</sup> Based on a 10-yr record from 1993 to 2002.

the monsoon season (3 months). About 60% of the annual discharge and 85% of the annual sediment flux occurs during the summer monsoon months June to August. A total of  $7.1 \cdot 10^5$  t/yr sediment is carried by the Baspa River, which corresponds to 937 t/(yr km<sup>2</sup>) for the drainage area (757 km<sup>2</sup>). We then estimate mean basin-denudation rates by applying a density for the suspended sediment of 1.4 t/m<sup>3</sup> to convert mass into volume. Mean basin denudation in the Baspa catchment is  $\sim 0.7 \pm 0.14$  mm/yr, while during the 2002 AMY, the rate more than doubled to  $\sim 1.5$  mm/yr. We emphasize that these values represent only minimum mean basin denudation rates, because bed-load transport has not been included and suspended sediment transport was not measured continuously during the 2002 monsoon season. In addition, we assumed a low bulk density for the suspended sediment and thus only considered a small fraction of the transported sediment in suspension. However, the differences in rates clearly demonstrate the impact of AMYs on mean basin lowering in the high-elevation parts of the northwestern Himalaya.

We relate enhanced sediment flux in the fluvial system to enhanced erosional slope processes that result from heavy rainfall. For example, representative

for enhanced hillslope erosion in this region, a large debris flow was triggered during several hours of heavy rainfalls in the Baspa Valley at the end of August 2002. The debris flow traveled from high elevation and carved a preexisting channel within the village of Sangla (Fig. 6). Numerous similar observations were made in the neighboring Sutlej, Rupa, and Spiti valleys. In these locations, the AMY-related rainfall primarily affected vegetation-free hillslopes, increased pore-water pressure, and destabilized steep, regolith-mantled slopes that eventually generated debris flows.

From laboratory, field, and theoretical studies of sediment transport mechanics, it is well known that sediment transport by free-surface flow, seepage, and shallow mass movements does not occur until a threshold of flow strength is exceeded (e.g., [40]). More recently, studies of watersheds in the western United States support the theory originally proposed by Horton [41] that a similar erosion threshold also controls the location of channel heads in some drainage basins (e.g., [42,43]). These studies suggest that channels form where the shear stress generated by surface flow during storms exceeds the threshold to entrain and transport sediment particles.

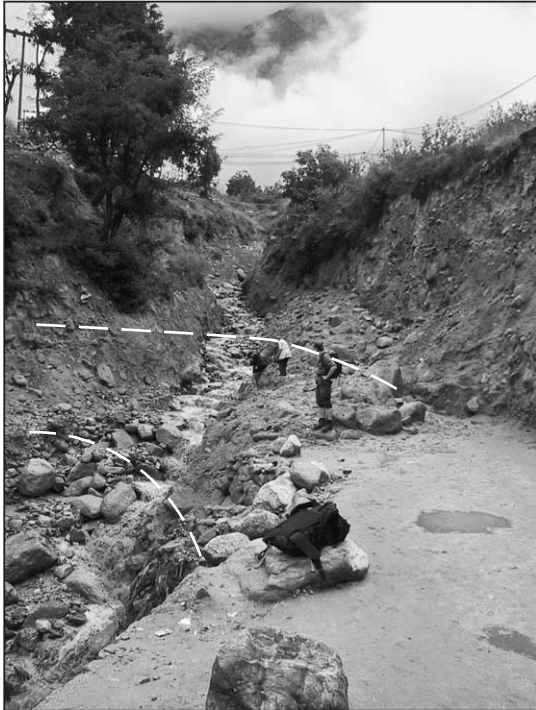


Fig. 6. Remnants of a debris-flow in the village of Sangla, Baspa Valley during the 2002 AMY (31.8.2002). White dashed lines indicate location of destroyed road. Note levee material related to debris flow showing the thickness of the flow.

During the 2002 AMY, the threshold of flow strength was clearly exceeded along scarcely vegetated, steep hillslopes in arid and semi-arid regions of the Himalaya, and new channel formation in the headwaters through debris flows could be observed. If new channel formation during extreme climate events is regionally relevant, then the extent of the channel network should be particularly sensitive to changes in climate (e.g., [44]). To assess the spatial distribution of new channel formation, we compared the three VNIR (Visible Near Infra Red) bands of the ASTER sensor taken before and after the 2002 AMY, on April 9 (Fig. 7A,C) and December 8 (Fig. 7B,D), respectively. In order to enhance output quality, sharpen the image, and reduce dimensionality, we applied principal component analysis (PCA) on the three input bands and show only the first component. The PCA rotates the input bands and aligns them along their axes of highest variance (e.g., [32]). Newly formed and eroded pre-existing channels on these false-color images have a

higher reflectance and data variance. Thus, PCA represents a tool to identify recently active areas. We circled and identified changes in the satellite images taken in December after the 2002 AMY (Fig. 7B,D; see electronic Appendix for additional information). In the field we found these channels to be the transport tracks for debris from the hillslopes. Despite the 15-m spatial resolution of the VNIR bands of ASTER images, we primarily observe reactivated and limited newly incised channels through debris flows. Not all flows reached the main stem and thus did not immediately supply more sediment to the river. An increase in debris flow activity in the arid, high-elevation part, was not observed during the previous normal ISM seasons, and also not in the HSP region during the AMY. Despite the imaginable inactivity of old channels during normal ISM conditions, we observe that they funnel even small amounts of runoff during weaker monsoon years. Thus, the initiation, carving, and reactivation of channels increases the erosion potential through collecting runoff and potentially focusing erosion during normal monsoon years in small parts of the hillslopes (e.g., [44]).

Based on these observations, we refer to the arid to semi-arid region as a geomorphic threshold area, where scarcely vegetated, steep hillslopes and channel networks are very sensitive to climatic changes (e.g., [42,44]). The rainfall threshold that triggers shallow hillslope erosion therefore lies between 0.3 m/yr and 0.7 m/yr. In contrast, the humid, vegetated medium-elevation regions do not show a significant increase in hillslope processes during the same time period. We argue that the dense, protective organic layer effectively intercepts precipitation and possibly reduces direct runoff and thus armors these environments. Although we observe a moderate increase in rainfall in these HSP regions and Sutlej River discharge during the 2002 AMY, a comparable increase in sediment flux did not take place compared to the high-elevation LSP compartment. Thus, increased material was derived from the arid, high-elevation areas, although presenting only a fraction of total sediment transport to the foreland basins during the 2002 AMY. Analogous to present-day conditions produced by AMYs, this phenomenon may have been much more pronounced during longer-lasting intensified monsoon phases in the geologic past (e.g., [11,45,46]).

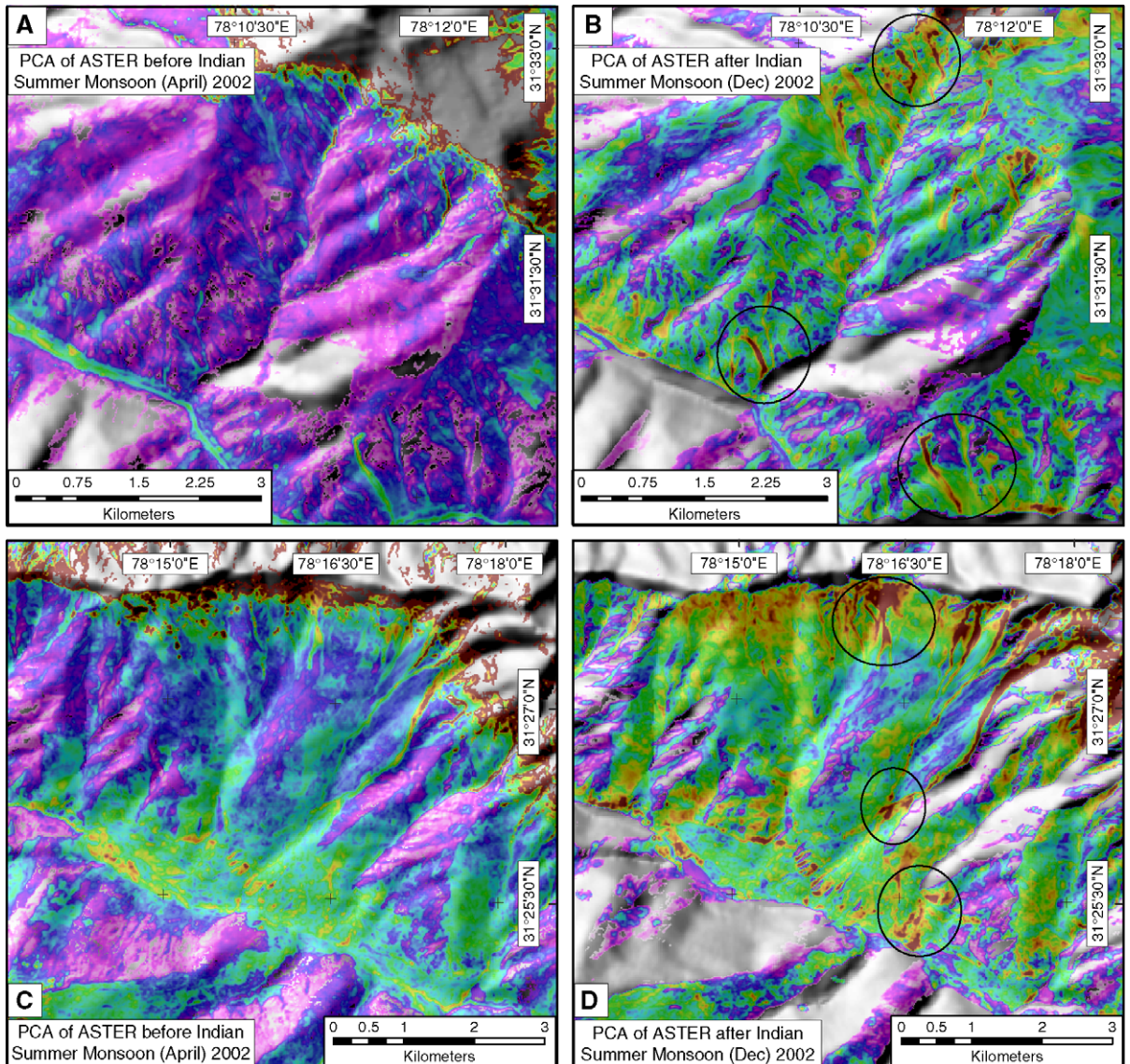


Fig. 7. Principal Component analysis (PCA) of ASTER Images before (April 9, A and C) and after (December 8, B and D) the 2002 AMY event (location shown on Fig. 4). Prior to PCA, the satellite data have been filtered to show more contrast by removing shadows and large snow fields along the peaks. We show the first axis of PCA that aligns along the highest variance of the all three input bands. Purple, blue, and green colors indicate low variance, whereas rivers, newly formed, and reactivated channels along the hillslopes have higher reflectance values (brown colors). Black circles outline newly formed or reactivated debris flow. These false-color images do not represent the original, natural color, and are draped over shaded-relief topography.

While we spatially linked moisture transport and erosion process distribution in detail during the 2002 AMY, we were also able to identify similar, extreme events during the last century. For example, Sangla ISM rainfall rates in the Baspa Valley (Fig. 4) indicate conditions similar to the 2002 AMY in 1957, 1968,

1978, and weaker event in 1990 (B.B.M.B., unpublished company data and [30]). Baspa discharge is available since 1965 and also shows significantly increased river discharge in AMYs (B.B.M.B., unpublished company data; Fig. 4). If a decadal recurrence interval is assumed, the influence of these

abnormal monsoon years on mean basin denudation is roughly 20% in the arid parts of the Sutlej Valley. However, high-resolution satellite observations unfortunately do not exist for earlier events and we are unable to reconstruct detailed moisture transport for this time. Although the mechanistic principle underlying these short-term climatic perturbations is not yet well understood and is a matter of ongoing debate (e.g., [12,34,47]), the potential effect of extreme monsoon events on erosional surface processes and their impact on sediment production is evident, resulting in effective hillslope erosion and increased sediment evacuation. This causative relationship in turn, may explain the higher sediment transport to the Bay of Bengal during longer-lasting intensified monsoon phases in the younger geologic past and may represent an important process in the erosion of the Himalayan orogen (e.g., [11,12]).

Despite active seismicity in the Himalaya and the possible seismic triggering of large landslide masses (e.g., [48]), earthquakes apparently only play a minor role in directly supplying increased sediment amounts to rivers in regions with strong monsoon seasons (e.g., [9,49,50]). Although comparison to other studies is difficult due to the complex geologic setting, Barnard et al. [9] examined sediment flux during the monsoon season in 2000 and after the  $M_s$  6.6 1999 earthquake in Garhwal, ~150 km E of the Sutlej Valley. Surprisingly, only a small overall contribution of earthquake-induced vs. monsoon-triggered mass transport was detected. Similar results were obtained by Owen et al. [49] after the  $M_s$  7.0 1991 Garhwal earthquake. Their study showed that equivalent landscape lowering due to earthquake- and rainfall-induced mass movements was ~0.007 and 0.02 mm, respectively. However, it may be cautioned that there might be a time lag between earthquake-induced processes and sediment removal during major precipitation events, thus considerably delaying sediment transport to lower elevations [51]. However, similar to other tectonically active orogens, it can be assumed that earthquakes are an important factor for sediment production in the humid, medium-elevation regions [50]. In any case, our results imply that denudation and more importantly, erosional hillslope processes in the arid, high-elevation regions of the Himalaya are strongly controlled by extreme storm events during abnormal monsoon years.

### **3. Conclusion**

We investigated synoptic and valley-scale precipitation gradients in the Himalayas using passive microwave data. Moisture is transported from the Bay of Bengal along the Southern Himalayan Mountain Front to the northwest and results in E–W and N–S precipitation gradients. Topography exerts a strong control on rainfall along the mountainous regions and during enhanced monsoonal circulation. In this event, deeply incised river valleys oriented normal to the Himalayan arc provide thoroughfares for moist air to be carried into arid areas of the orogen. Interannual variations in precipitation penetration strongly depend on the characteristics of the Indian Summer Monsoon circulation. For the year 2002, we identified an abnormal monsoon year (AMY) for the northwest Himalaya, when rain migrated far into the orogen and reached regions shielded by orographic barriers. These typically arid sectors are characterized by steep, sparsely vegetated, and regolith-mantled hillslopes, and represent geomorphic threshold areas. During abnormal strong rainfall events, these slopes respond with enhanced erosional processes. We identify debris flows in the upper catchment regions as effective geomorphic erosion agents that are triggered by unusually high rainfall intensities. Suspended sediment transport measurements reveal that more than twice as much sediment may be evacuated by rivers in these dry regions of the orogen during high climatic variations. The increased sediment load in mountain streams documents significantly enhanced mean basin denudation rates in the arid sectors of the northwest Himalaya. In contrast, the low- to medium-elevation portions of the orogen are characterized by smaller rainfall-magnitude changes during the AMY, and do not show increased but overall high denudation rates. We argue that this might be a result of the protective organic layer that effectively intercepts precipitation and modulates runoff on densely vegetated slopes. While we documented the relationship between the migration of precipitation far into the orogen and sediment production processes only in the northwest Himalaya, we suggest that similar processes also occur along the entire southern Himalayan mountain front, where topographic barriers allow penetration of moisture to higher-elevation, arid sectors.

## Acknowledgements

This work was supported by the German Research Foundation (DFG STR371/11-1). The success of this project was made possible through the support of many Indian friends and colleagues. We particularly thank A.K. Jain and S. Singh, both of I.I.T. Roorkee, India for their help. We gratefully acknowledge K. Haselton for his support on SSM/I data processing. We thank P. van der Beek, D. Burbank, B. Dietrich, and N. Hovius for constructive reviews and discussions. Daily sediment transport and river discharge measurements were provided by Dr. Narendra Singh of Jaiprakash Hydroelectric Power Industries Limited, New Delhi (India) for the Baspa River, a major tributary of the Sutlej. We appreciate discussions with L. Schoenbohm and E. Sobel. SSM/I and ASTER data were obtained from the NASA Pathfinder Program for early Earth Observing System (EOS) products.

## Appendix A. Supplementary data

Supplementary data associated with this article can be found, in the online version, at doi:10.1016/j.epsl.2004.11.014.

## References

- [1] V.R. Baker, V.S. Kale, The role of extreme floods in shaping bedrock channels, in: K.J. Tinkler, E.E. Wohl (Eds.), *Rivers over rock: fluvial processes in bedrock channels*, Geophys. Monogr. Ser., vol. 107, AGU, Washington, DC, 1998, pp. 153–165.
- [2] S.J. Dadson, N. Hovius, H.G. Chen, W.B. Dade, M.L. Hsieh, S.D. Willett, J.C. Hu, M.J. Horng, M.C. Chen, C.P. Stark, D. Lague, J.C. Lin, Links between erosion, runoff variability and seismicity in the Taiwan orogen, *Nature* 426 (6967) (2003) 648–651.
- [3] R. Coppus, A.C. Imeson, Extreme events controlling erosion and sediment transport in a semi-arid sub-Andean valley, *Earth Surf. Processes Landf.* 27 (13) (2002) 1365–1375.
- [4] K. Hartshorn, N. Hovius, W.B. Dade, R.L. Slingerland, Climate-driven bedrock incision in an active mountain belt, *Science* 297 (5589) (2002) 2036–2038.
- [5] P. Molnar, P. England, Late Cenozoic uplift of mountain-ranges and global climate change—chicken or egg, *Nature* 346 (6279) (1990) 29–34.
- [6] N.P. Snyder, K.X. Whipple, G.E. Tucker, D.J. Merritts, Importance of a stochastic distribution of floods and erosion thresholds in the bedrock river incision problem, *J. Geophys. Res., [Solid Earth]* 108 (B2) (2003) 17-1–17-15 (art. no.-2117).
- [7] S.K. Paul, S.K. Bartarya, P. Rautela, A.K. Mahajan, Catastrophic mass movement of 1998 monsoons at Malpa in Kali Valley, Kumaun Himalaya (India), *Geomorphology* 35 (3–4) (2000) 169–180.
- [8] M.P. Sah, R.K. Mazari, Anthropogenically accelerated mass movement, Kulu Valley, Himachal Pradesh, India, *Geomorphology* 26 (1–3) (1998) 123–138.
- [9] P.L. Barnard, L.A. Owen, M.C. Sharma, R.C. Finkel, Natural and human-induced landsliding in the Garhwal Himalaya of northern India, *Geomorphology* 40 (1–2) (2001) 21–35.
- [10] F. Gasse, M. Arnold, J.C. Fontes, M. Fort, E. Gibert, A. Huc, B.Y. Li, Y.F. Li, Q. Lju, F. Melieres, E. Vancampo, F.B. Wang, Q.S. Zhang, A 13,000-year climate record from western Tibet, *Nature* 353 (6346) (1991) 742–745.
- [11] B. Bookhagen, R.C. Thiede, M.R. Strecker, Late Quaternary intensified monsoon phases control landscape evolution in the northwest Himalaya, *Geology* (in press).
- [12] S. Gadgil, The Indian monsoon and its variability, *Annu. Rev. Earth Planet. Sci.* 31 (2003) 429–467.
- [13] P.J. Webster, L.C. Chou, Seasonal structure of a simple monsoon system, *J. Atmos. Sci.* 37 (2) (1980) 354–367.
- [14] P.J. Webster, V.O. Magaña, T.N. Palmer, J. Shukla, R.A. Tomas, M. Yanai, T. Yasunari, Monsoons: processes, predictability, and the prospects for prediction, *J. Geophys. Res., [Oceans]* 103 (C7) (1998) 14451–14510.
- [15] C.D. Charles, D.E. Hunter, R.G. Fairbanks, Interaction between the ENSO and the Asian monsoon in a coral record of tropical climate, *Science* 277 (5328) (1997) 925–928.
- [16] C.O. Clark, J.E. Cole, P.J. Webster, Indian Ocean SST and Indian summer rainfall: predictive relationships and their decadal variability, *J. Climate* 13 (14) (2000) 2503–2519.
- [17] M.L. Shrestha, Interannual variation of summer monsoon rainfall over Nepal and its relation to Southern Oscillation Index, *Meteorol. Atmos. Phys.* 75 (1–2) (2000) 21–28.
- [18] T.J. Lang, A.P. Barros, An investigation of the onsets of the 1999 and 2000 monsoons in central Nepal, *Mon. Weather Rev.* 130 (5) (2002) 1299–1316.
- [19] A.P. Barros, D.P. Lattenmaier, Dynamic modeling of orographically induced precipitation, *Rev. Geophys.* 32 (3) (1994) 265–284.
- [20] R.B. Smith, Some aspects of the quasi-geostrophic flow over mountains, *J. Atmos. Sci.* 36 (12) (1979) 2385–2393.
- [21] J.P. Hollinger, Special issue on the defense meteorological satellite program (Dmsp-Calibration and Validation of the Special Sensor Microwave Imager (Ssm/I)), *IEEE Trans. Geosci. Remote Sens.* 28 (5) (1990) 779–780.
- [22] N.C. Grody, Classification of snow cover and precipitation using the special sensor microwave imager, *J. Geophys. Res., [Atmos.]* 96 (D4) (1991) 7423–7435.
- [23] R.R. Ferraro, Special sensor microwave imager derived global rainfall estimates for climatological applications, *J. Geophys. Res., [Atmos.]* 102 (D14) (1997) 16715–16735.
- [24] C. Kummerow, L. Giglio, A passive microwave technique for estimating rainfall and vertical structure information from

- Space: 1. Algorithm description, *J. Appl. Meteorol.* 33 (1) (1994) 3–18.
- [25] C. Kummerow, L. Giglio, A passive microwave technique for estimating rainfall and vertical structure information from Space: 2. Applications to Ssm/I Data, *J. Appl. Meteorol.* 33 (1) (1994) 19–34.
- [26] R.R. Ferraro, E.A. Smith, W. Berg, G.J. Huffman, A screening methodology for passive microwave precipitation retrieval algorithms, *J. Atmos. Sci.* 55 (9) (1998) 1583–1600.
- [27] T.T. Wilheit, R. Adler, S. Avery, E. Barrett, P. Bauer, W. Berg, A. Chang, J. Ferriday, N. Grody, S. Goodman, C. Kidd, D. Kniveton, C. Kummerow, A. Mugnai, W. Olson, G. Petty, A. Shibata, E. Smith, R. Spencer, Algorithms for the retrieval of rainfall from passive microwave measurements, *Remote Sens. Rev.* 11 (1994) 163–194.
- [28] G.W. Petty, The status of satellite-based rainfall estimation over land, *Remote Sens. Environ.* 51 (1) (1995) 125–137.
- [29] A.P. Barros, M. Joshi, J. Putkonen, D.W. Burbank, A study of the 1999 monsoon rainfall in a mountainous region in central Nepal using TRMM products and rain gauge observations, *Geophys. Res. Lett.* 27 (22) (2000) 3683–3686.
- [30] T.C. Peterson, R.S. Vose, An overview of the global historical climatology network temperature database, *Bull. Am. Meteorol. Soc.* 78 (12) (1997) 2837–2849.
- [31] M.R. Bhutiyani, Sediment load characteristics of a proglacial stream of Siachen Glacier and the erosion rate in Nubra valley in the Karakoram Himalayas, India, *J. Hydrol.* 227 (1–4) (2000) 84–92.
- [32] J.A. Richards, Remote sensing digital image analysis: an introduction, Springer-Verlag, Berlin, Germany, 1994, 340 pp.
- [33] B. Parthasarathy, K.R. Kumar, D.R. Kothawale, Indian-summer monsoon rainfall indexes—1871–1990, *Meteorol. Mag.* 121 (1441) (1992) 174–186.
- [34] J.M. Slingo, H. Annamalai, 1997: The El Niño of the century and the response of the Indian summer monsoon, *Mon. Weather Rev.* 128 (6) (2000) 1778–1797.
- [35] K.V. Hodges, C. Wobus, K. Ruhl, T. Schildgen, K. Whipple, Quaternary deformation, river steepening, and heavy precipitation at the front of the Higher Himalayan ranges, *Earth Planet. Sci. Lett.* 220 (3–4) (2004) 379–389.
- [36] R.C. Thiede, B. Bookhagen, J.R. Arrowsmith, E.R. Sobel, M.R. Strecker, Climatic Control on rapid exhumation along the Southern Himalayan Front, *Earth Planet. Sci. Lett.* 222 (3–4) (2004) 791–806.
- [37] M.G. Wolman, J.P. Miller, Magnitude and frequency of forces in geomorphic processes, *J. Geol.* 68 (1) (1960) 54–74.
- [38] M. Mulligan, Modelling the geomorphological impact of climatic variability and extreme events in a semi-arid environment, *Geomorphology* 24 (1) (1998) 59–78.
- [39] W.R. Osterkamp, J.M. Friedman, The disparity between extreme rainfall events and rare floods—with emphasis on the semi-arid American West, *Hydrol. Process.* 14 (16–17) (2000) 2817–2829.
- [40] M.S. Yalin, Mechanics of sediment transport, 2nd ed., Pergamon, Tarrytown, NY, 1977, 298 pp.
- [41] R.E. Horton, Erosional development of streams and their drainage basins: hydrophysical approach to quantitative morphology, *Bull. Geol. Soc. Am.* 56 (1945) 275–370.
- [42] D.R. Montgomery, W.E. Dietrich, Channel initiation and the problem of landscape scale, *Science* 255 (5046) (1992) 826–830.
- [43] W.E. Dietrich, C.J. Wilson, D.R. Montgomery, J. McKean, R. Bauer, Erosion thresholds and land surface-morphology, *Geology* 20 (8) (1992) 675–679.
- [44] G.E. Tucker, R. Slingerland, Drainage basin responses to climate change, *Water Resour. Res.* 33 (8) (1997) 2031–2047.
- [45] B. Pratt, D.W. Burbank, A. Heimsath, T. Ojha, Impulsive alluviation during early Holocene strengthened monsoons, central Nepal Himalaya, *Geology* 30 (10) (2002) 911–914.
- [46] S.L. Goodbred, S.A. Kuehl, Enormous Ganges–Brahmaputra sediment discharge during strengthened early Holocene monsoon, *Geology* 28 (12) (2000) 1083–1086.
- [47] P.J. Webster, A.M. Moore, J.P. Loschnigg, R.R. Leben, Coupled ocean–atmosphere dynamics in the Indian Ocean during 1997–98, *Nature* 401 (6751) (1999) 356–360.
- [48] D.K. Keefer, The importance of earthquake-induced landslides to long-term slope erosion and slope-failure hazards in seismically active regions, *Geomorphology* 10 (1–4) (1994) 265–284.
- [49] L.A. Owen, M. Sharma, R. Bigwood, Landscape modification and geomorphological consequences of the 20 October 1991 earthquake and the July–August 1992 monsoon in the Garhwal Himalaya, *Z. Geomorphol.* 103 (1996) 359–372.
- [50] N. Hovius, C.P. Stark, H.T. Chu, J.C. Lin, Supply and removal of sediment in a landslide-dominated mountain belt: Central Range, Taiwan, *J. Geol.* 108 (1) (2000) 73–89.
- [51] J. Lavé, D.W. Burbank, Denudation processes and rates in the Transverse Ranges, southern California: erosional response of a transitional landscape to external and anthropogenic forcing, *J. Geophys. Res., [Surface]* 109 (F01006) (2004).